Biochemical and Biophysical Research Communications 374 (2008) 134–137

Contents lists available at ScienceDirect

Biochemical and Biophysical Research Communications

journal homepage: www.elsevier.com/locate/ybbrc

Inactive S298R disassembles the dodecameric L-aspartate 4-decarboxylase into dimers

Nai-Chen Wang [a], Tzu-Ping Ko [b], Chia-Yin Lee [a,*]

[a] Department of Agricultural Chemistry, National Taiwan University, 1, Section 4, Roosevelt Road, Taipei 10617, Taiwan
[b] Institute of Biological Chemistry, Academia Sinica, Taipei 11529, Taiwan

ARTICLE INFO

Article history:
Received 20 June 2008
Available online 3 July 2008

Keywords:
L-Aspartate 4-decarboxylase
Protein assembly
Mutagenesis
Computer modeling

ABSTRACT

L-Aspartate 4-decarboxylase catalyzes the conversion of aspartate to alanine and CO_2. The wild-type enzyme was observed as dodecamers at pH 5.0. The mutation of Ser298 into Arg resulted in an almost complete loss of the enzyme activity, and caused regional structural distortion and defects in the enzyme assembly, as shown in circular dichroism spectra and gel filtration profiles. Mutating Tyr207 and Pro257 into His also resulted in inactivation of the enzyme, but did not affect the overall structure. Computer modeling suggests that Ser298 is located on the surface, and its mutation may result in enzyme disassembly, whereas Tyr207 and Pro257 are near the active site, and their mutations may cause local structure perturbation.

L-Aspartate 4-decarboxylase (Asd; EC 4.1.1.12) catalyzes the decarboxylation of L-aspartate to produce L-alanine. This enzyme has been found only in a limited number of microorganisms including eubacteria, actinomycetes, and fungi [1–7]. Regardless of the enzyme sources, the optimal pH for its activity is around pH 5 [2,3,7] even when it catalyzes the desulfination reaction of cysteine sulfinic acid [8]. This enzyme catalyzes not only the β-elimination reactions, but also a low degree of transamination between several L-amino acids and α-keto acids [9]. Both reactions exhibited the highest activity at pH 4.5–5.5 [3]. Proton concentration was shown to affect the quaternary structure of the enzyme [10–12]. As derived from the previous results of sedimentation experiments, six dimers of the *Alcaligenes* enzyme assembled into a dodecamer at pH 5.0 [11], and this holoenzyme dissociated into an apoenzyme at pH 8.0. The holoenzyme can also be restored by treatment with its cofactor, pyridoxal 5′-phosphate (PLP) [10]. Similar re-association was also observed with the enzyme from *Pseudomonas dacunhae* [12].

The PLP-enzymes, with a great versatility, have been classified into several families, according to the different protein folds [13]. Type I enzymes, to which Asd belongs, contain a PLP-binding domain with a central β-strand surrounded by several α-helices. We have produced several mutants that exhibited altered bifunctional catalytic activity [14]. Three of the single-site mutants at Tyr207, Pro257, and Ser298 were completely inactive. To investigate the cause of inactivation by these mutants, circular dichroism and gel filtration were used to characterize them. Furthermore, as we have noted, Asd contains a region of the type I PLP-binding motif [15]. Based on a three-dimensional model constructed for this region, the importance of the three inactivating amino acid residues is discussed.

Materials and methods

Strains, media, and chemicals. Escherichia coli XL1-Blue (Stratagene) and *E. coli* BL21(DE3)pLysS (Novagen) were used as hosts for gene propagation and expression, respectively. Plasmids were prepared by GenElute Plasmid Miniprep kit (Sigma). *Escherichia coli* cells were grown aerobically at 35 °C in Luria–Bertani broth with antibiotics as required (100 μg/ml ampicillin and 34 μg/ml chloramphenicol). Chemicals used in this study were purchased mainly from Sigma.

Mutant construction and purification of the recombinant enzyme. The asd gene that encodes *Pseudomonas* sp. ATCC 19121 Asd was constructed in a pET expression system as described previously [15]. This gene was mutated with the QuikChange Site-Directed Mutagenesis kit (Stratagene) and then expressed in *E. coli* BL21(DE3)pLysS. Forward mutagenic primers used to generate *asd* mutants are: Y207H 5′-GGTGTTCACGCCGCATATCGAGATCCC-3′, P256H 5′-GTGAACCCCAGCAACATGCCGTCCGTGAAGATG-3′, S298R 5′-GCCGATGAATTCCAGCGCCTTTTCTCGGTCTGC-3′ (mutated codons are underlined). The isopropyl-β-D-thiogalactopyranoside induced cells were disrupted by ultrasonication (model XL2020, Misonix). Cell extracts were clarified by centrifugation, and the resulting supernatants were purified with a HiTrap Chelating column (GE) as described

* Corresponding author. Fax: +886 2 23660581.
E-mail address: clee@ntu.edu.tw (C.-Y. Lee).

0006-291X/$ - see front matter © 2008 Elsevier Inc. All rights reserved.
doi:10.1016/j.bbrc.2008.06.110

previously [15]. The purified enzyme was analyzed by sodium dodecyl sulfate–polyacrylamide gel electrophoresis (SDS–PAGE) and verified by Western blot analysis using polyclonal anti-Asd antisera as in our previous study [14]. Amino acid residues are numbered according to the sequence of Asd from *Alcaligenes faecalis* CCRC 11585 (Accession No. AAK58507) [16].

Enzyme assays. Five micrograms of purified enzyme was added to a reaction mixture (500 μl) containing 40 mM α-ketoglutarate, 0.5 mM PLP, and 40 mM L-aspartate in 0.3 M acetate buffer (pH 5.0) to start the enzyme reaction, which was then stopped by boiling after 20 min. Protein was precipitated by treatment with 5-sulfosalicylic acid (2%), cooling at 4 °C for 30 min, and centrifuging at 15,000 rpm for 20 min. Amino acids in the supernatant were derivatized with *o*-phthaldialdehyde (OPA) reagent solution (Sigma) and analyzed with a LichroCART RP-18 column (5 μm, 250 × 4.6 mm, Merck) by high-performance liquid chromatography (HPLC) as described by Jones and Gilligan [17]. Protein concentration was determined by the Bradford method using bovine serum albumin as the standard [18]. One unit of Asd activity was defined as the amount of enzyme that catalyzes the production of 1 μmol of alanine (or glutamate for transaminase activity) per min at 37 °C.

Circular dichroism spectroscopy. The purified enzyme was concentrated with Amicon Ultra (10,000 MWCO) (Millipore) and exchanged into 10 mM sodium phosphate buffer (pH 6.0) in a final concentration of 2 μM. CD spectra were taken over a range of 190–250 nm at 0.1 nm increments and a 0.25 s acquisition time on a Jasco J-715 CD spectropolarimeter (Japan). Each protein sample with 0.1 mM PLP was scanned in a 1-mm quartz cuvette three times with 10 mdeg sensitivity. The CD spectra were analyzed by CDSSTR method at Dichroweb [19].

Gel filtration analysis. The purified Asd was eluted at the rate of 0.5–0.8 ml/min with 0.1 M sodium acetate buffer (pH 5.0) containing 0.2 M NaCl, with a HiPrep 16/60 Sephacryl S-300 HR column (GE Healthcare) by fast protein liquid chromatography (AKTA FPLC, GE Healthcare) to determine the oligomeric state of the Asd. Molecular weights of eluted proteins were calculated according to the regression curve of log (molecular weight) vs. retention time of each protein standard (MW-GF-1000, Sigma), and ranged from 29 to 2000 kDa, as measured.

Computer modeling. The atomic coordinates of PDB 3TAT (A chain) for *E. coli* tyrosine aminotransferase (TAT) [20] were used as a template. Only the PLP-binding domain shows a significant number of identical residues and no large gaps in the aligned sequences. The similarity of the entire sequences between Asd and TAT is 28%. However, the similarity of the PLP-binding domains between Asd and TAT is 34%. The few regions of deletions and insertions were manipulated using the program O [21], where the side chains were also substituted and adjusted. The model was expanded into a dimer similar to the TAT template and subjected to molecular dynamics and energy minimization using the program CNS [22].

Results

Enzyme inactivation by single-site mutations

To investigate important amino acid residues of the enzyme in catalytic activity, we constructed more than 20 point mutations by site-directed mutagenesis according to its sequence alignment with some aminotransferases and L-aspartase 4-decarboxylase [14]. All mutations were confirmed by sequencing, and the resultant enzymes were verified by Western blot (Fig. 1A, which shows only three of them). Three mutant enzymes, Y207H, P257H, and S298R, lost 99.9% of their decarboxylase activity and retained only about 10% of their aminotransferase activity (Table 1).

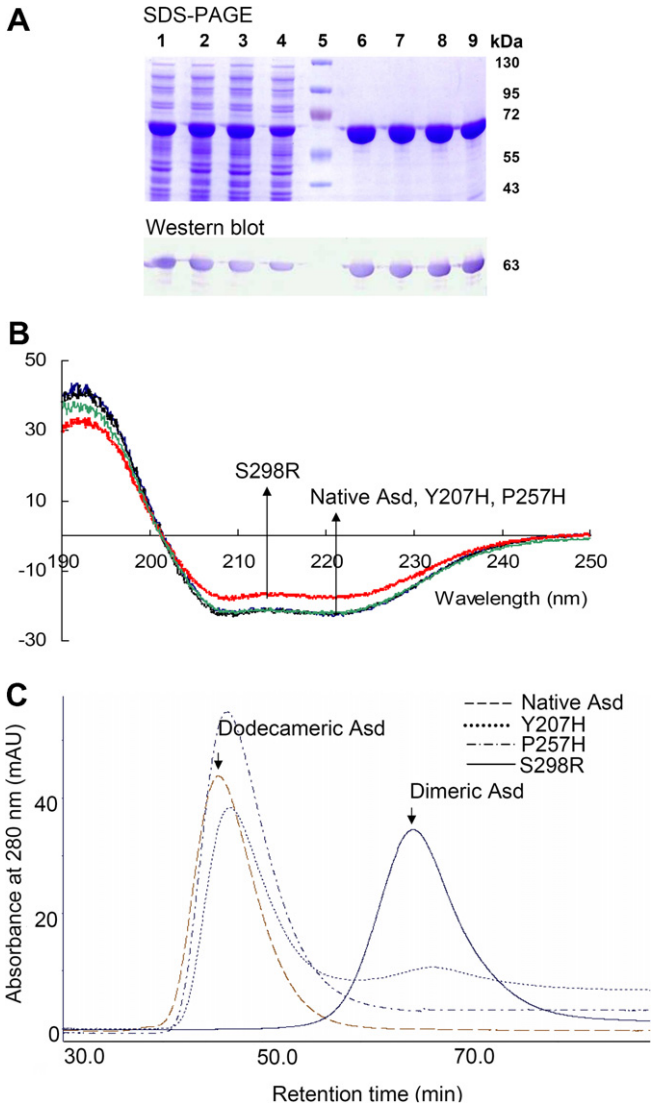

Fig. 1. Characterization of the native and mutant Asds. (A) Western analysis of the cell lysate and purified fractions of mutated His-tagged Asd. Lanes: 1 and 6, native Asd; 2 and 7, Y207H; 3 and 8, P257H; 4 and 9, S298R; 1–4, cell lysate; 5, molecular weight marker; 6–9, purified fractions. (B) Circular dichroism spectra in the far UV region. The protein concentration used was 2 μM in 10 mM phosphate buffer (pH 6.0) containing 0.1 mM PLP. In the peptide backbone region (205–230 nm), α-helix content increases for S298R as compared to the native enzyme. (C) Gel filtration profiles. Two milligrams of each protein was injected and eluted at a rate of 0.5 ml min^{-1}. Native Asd, Y207H, and P257H existed as dodecamers, where as S298R was seen as the dimer form, even at pH 5.0.

Influence of mutated amino acid residues on structure

The native and all three mutant enzymes were scanned for circular dichroism (CD) at the same protein concentration of 2 μM.

Table 1
Specific activities of Asd proteins in acetate buffer (pH 5.0) at 40 °C

Asd	Aspartate β-decarboxylation		Aspartate aminotransferation	
	Specific activity (U mg^{-1})	Relative activity (%)	Specific activity (U mg^{-1})	Relative activity (%)
Native	20.3 ± 1.2	100 ± 6.0	0.100 ± 0.005	100 ± 4.6
Y207H	0.02 ± 0.01	0.10 ± 0.05	0.009 ± 0.0004	9.0 ± 0.4
P257H	0.02 ± 0.01	0.08 ± 0.05	0.008 ± 0.001	8.5 ± 1.0
S298R	0.02 ± 0.01	0.08 ± 0.05	0.006 ± 0.001	6.0 ± 0.9

Table 2
Data analysis of circular dichroism spectra

Protein	α_R	α_D	Total α	β_R	β_D	Total β	Turn	Unordered	NRMSD
Wild type	0.39	0.21	0.60	0.04	0.04	0.08	0.13	0.20	0.009
Y207H	0.37	0.20	0.57	0.06	0.04	0.10	0.11	0.21	0.013
P257H	0.39	0.21	0.60	0.04	0.03	0.07	0.12	0.22	0.012
S298R	0.32	0.19	0.51	0.04	0.04	0.08	0.15	0.27	0.014

α_R, regular α-helix; α_D, distorted α-helix; β_R, regular β-strand; β_D, distorted β-strand; NRMSD, normalized root mean square deviation.

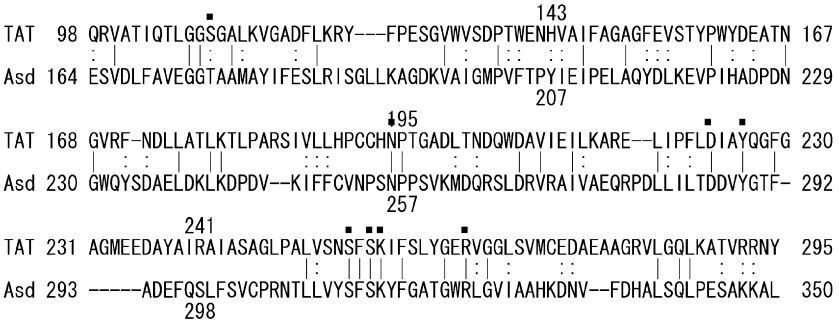

Fig. 2. Partial sequence alignment. The PLP-binding domain of tyrosine aminotransferase from *E. coli* K-12 (TAT) shows mediocre sequence homology to the putative PLP-domain of Asd from *Pseudomonas* sp. ATCC 19121 (Asd). Lines and colons denote identities and similarities, respectively. The three mutated sites and catalytically important residues are number- and square-labeled, respectively.

According to the CD spectra (Fig. 1B), the only mutation that affected enzyme structure was S298R. Since all these three mutants inactivated the enzyme, gel filtration analysis at pH 5.0 was carried out to verify if the lost activity was due to its assembly number of subunits. As shown in Fig. 1C, both native enzyme and the P257H mutant existed only as dodecamers at pH 5.0, whereas some dissociated dimers were observed in Y207H. The most striking phenomenon was observed for the S298R mutant protein, which existed only in dimeric form. The activity loss of S298R was probably due to overall structural changes as reflected in the CD spectra (Table 2).

The PLP-binding domain

The amino acid sequences of Asd from *Pseudomonas* sp. ATCC 19121 and Tyr aminotransferase (TAT) from *E. coli* K-12 have 18% identity and 34% similarity in the PLP-binding domain (Fig. 2), including the class I attachment site [14]. The *e*-value between PLP-binding domain of Asd from *Pseudomonas* sp. ATCC 19121 and that of TAT from *E. coli* sequence is 0.014. As shown in Fig. 3A, the model superimposes well with the TAT dimer, with an RMSD of 1.002 Å for 362 matched C_α atom. The *Z*-score calculated by the DALI server (http://www.ebi.ac.uk/dali) is 24.6. Configuration in the active site is mostly conserved, including the PLP-binding motif where Lys315 (258 in TAT) is covalently attached to the PLP, the charged Arg323 (266) and Asp286 (222), and a number of other polar residues that make direct hydrogen bonds with the PLP group, as shown in Fig. 3B. This model allowed us to derive possible locations of the three mutated amino acid residues of Tyr207, Pro257, and Ser298.

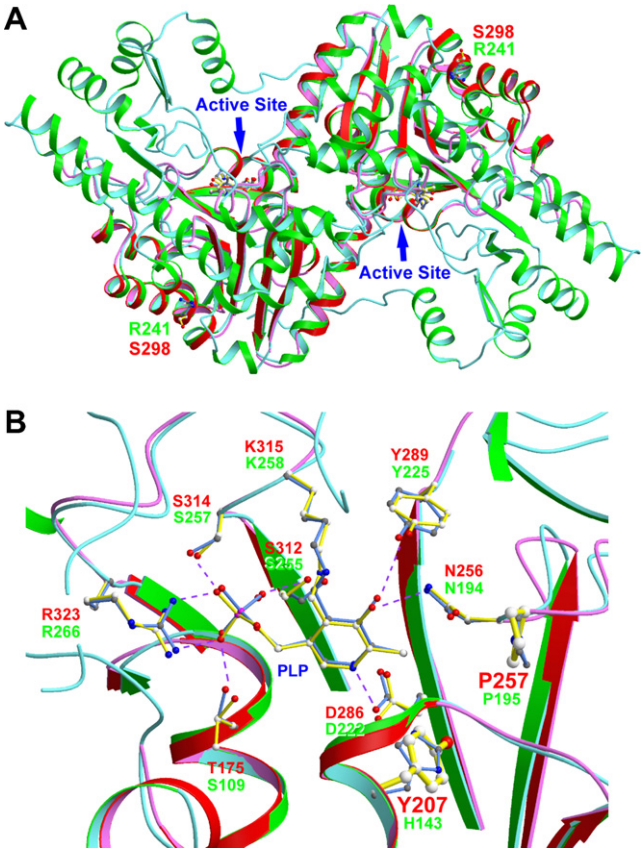

Fig. 3. Positions of the mutated residues predicted by computer modeling. (A) A model of the PLP-binding domains of Asd is shown as red and pink ribbons, superimposed on the dimeric overall structure of the TAT template (green and cyan). The active sites that contain bound PLP are indicated with arrows. The side chains of Arg241 of TAT and the predicted Ser298 of Asd are also shown. (B) Possible dispositions of the mutated residues of Tyr207 and Pro257 in Asd are shown as ball-and-stick models with thick yellow bonds, in the context of other predicted active-site residues (thin bonds). Blue bonds denote the equivalent residues in TAT. The hydrogen bonds observed in TAT are shown as dashed lines. The ribbons are colored as in (A). (For interpretation of the references to color in this figure legend, the reader is referred to the web version of this paper.)

Discussion

The three inactivated mutants (Y207H, P257H, and S298R) have varied effects on the enzyme assembly. By analyzing the CD spectra and gel filtration profiles of the mutants (Fig. 1), we found that the S298R mutation altered the protein's secondary structure (see also Table 2). The results of computer modeling suggested that Ser298 is probably located on a distal surface of the dimer (Fig.

3A), which might contribute to the packaging into dodecamers. The large positively charged side chain of Arg should have a significant structural impact on this interface. A previously studied mutant of D360P also showed comparable large changes in secondary structure, but it was observed as dodecamer at pH 5 and retained significant activity [14]. In contrast, the mutation of S298R in the enzyme rendered the dodecameric Asd enzyme disassembly, and caused inactivation. There seems to be a correlation among the proton concentration, the dodecamer assembly and the enzyme activity. In retrospect, an early elution was observed in the purification profile of S298R mutant with a nickel affinity column, which implied that there might be some structural impact of this mutant. However, further work is necessary to clarify the relationship.

On the other hand, Tyr207 and Pro257 are likely located in the vicinity of the active site (Fig. 3B). Although these two residues turned out to be quite important for catalytic activity, their mutations did not obviously affect the overall structure, as shown by the CD spectra (Fig. 1B). His143 in TAT does not interact directly with PLP; nor is it involved in catalysis, but mutating the equivalent Tyr207 in Asd to His resulted in loss of both decarboxylase and aminotransferase activities. Perhaps the phenolic oxygen is important in the maintenance of the active-site structure. It is noteworthy that Pro195 in TAT, which corresponds to Pro257 in Asd, has a cis-peptide configuration that is less common for non-proline residues (Fig. 3B).

The homology model of the PLP-binding domain of Asd from *Pseudomonas* sp. ATCC 19121 shows a conserved active-site configuration as in those of the well-studied aminotransferases. It provides a starting point for understanding the catalytic properties of the enzyme. According to CD spectral analysis, the entire protein structure of Asd has 60% α-helix and only 8% β-sheet (Table 2). Interestingly, the secondary structure contents of α-helices and β-strands in this PLP-binding domain region (Fig. 3B) are 40% and 30%, respectively. We found that deviate significantly from those estimated by the CD spectra for the total protein structure (Table 2). Probably, the other regions of the molecule contain more α-helices and fewer β-strands. Besides, the level of aminotransferase activity decreased less than that of the decarboxylase activity during the disrupted mutations (Table 1). These results indicated that the decarboxylase reaction would require a more stringent environment for catalysis, whereas the aminotransferase catalysis may still occur without the optimal environment (Fig. 3). We have used this model to explain the altered decarboxylase and aminotransferase activities in a recent study [14]. Regarding which amino acid residues are involved in subunit assembly, a more precise approach should be based on the crystalline structure of the enzyme. Although crystallization of Asd was first published in 1963 [2], its three-dimensional structure has not been determined by X-ray crystallography. Therefore, we have crystallized the Asd enzyme, and we are going to solve its structure in the near future.

Acknowledgments

We are grateful to Drs. Andrew H.-J. Wang and Hui-Chuan Chang in the Institute of Biological Chemistry, Academia Sinica, Taiwan, for their assistance with obtaining the CD spectra. This work was supported by the National Science Council of Taiwan under the Grants NSC94-2313-B-002-049 and NSC95-2811-B-002-055 and partly by the Frontier and Innovative Research of National Taiwan University Project No. 95R0105.

References

[1] A. Meister, H.A. Sober, S.V. Tice, Enzymatic decarboxylation of aspartic acid to α-alanine, J. Biol. Chem. 189 (1951) 577–590.
[2] E.M. Wilson, H.L. Kornberg, Properties of crystalline L-aspartate 4-carboxy-lyase from *Achromobacter* sp., Biochem. J. 88 (1963) 578–587.
[3] A. Novogrodsky, A. Meister, Control of aspartate β-decarboxylase activity by transamination, J. Biol. Chem. 239 (1964) 879–888.
[4] I. Chibata, T. Kakimoto, J. Kato, Enzymatic production of L-alanine by *Pseudomonas dacunhae*, Appl. Microbiol. 13 (1965) 638–645.
[5] K. Abe, F. Ohnishi, K. Yagi, T. Nakajima, T. Higuchi, M. Sano, M. Machida, R.I. Sarker, P.C. Maloney, Plasmid-encoded *asp* operon confers a proton motive metabolic cycle catalyzed by an aspartate–alanine exchange reaction, J. Bacteriol. 184 (2002) 2906–2913.
[6] L.V. Crawford, Studies on the aspartic decarboxylase of *Nocardia globerula*, Biochem. J. 68 (1958) 221–225.
[7] T.A. El-Rahmany, Comparison of L-aspartate 4-carboxy-lyases of *Cunninghamella elegans* and *Penicillium citrinum*, Microbiol. Res. 149 (1994) 253–257.
[8] K. Soda, A. Novogrodsky, A. Meister, Enzymatic desulfination of cysteine sulfinic acid, Biochemistry 3 (1964) 1450–1454.
[9] A. Novogrodsky, J.S. Nishimura, A. Meister, Transamination and β-decarboxylation of aspartate catalyzed by the same pyridoxal phosphate-enzyme, J. Biol. Chem. 238 (1963) PC1903–PC1905.
[10] S.S. Tate, A. Meister, Studies on the sulfhydryl groups of L-aspartate β-decarboxylase, Biochemistry 7 (1968) 3240–3247.
[11] W.F. Bowers, V.B. Czubaroff, R.H. Haschemeyer, Subunit structure of L-aspartate β-decarboxylase from *Alcaligenes faecalis*, Biochemistry 9 (1970) 2620–2625.
[12] S.S. Tate, A. Meister, Regulation and subunit structure of aspartate β-decarboxylase. Studies on the enzymes from *Alcaligenes faecalis* and *Pseudomonas dacunhae*, Biochemistry 9 (1970) 2626–2632.
[13] J.N. Jansonius, Structure, evolution and action of vitamin B6-dependent enzymes, Curr. Opin. Struct. Biol. 8 (1998) 759–769.
[14] N.C. Wang, C.Y. Lee, Enhanced transaminase activity of a bifunctional L-aspartate 4-decarboxylase, Biochem. Biophys. Res. Commun. 356 (2007) 368–373.
[15] N.C. Wang, C.Y. Lee, Molecular cloning of the aspartate 4-decarboxylase gene from *Pseudomonas* sp. ATCC 19121 and characterization of the bifunctional recombinant enzyme, Appl. Microbiol. Biotechnol. 73 (2006) 339–348.
[16] C.C. Chen, T.L. Chou, C.Y. Lee, Cloning, expression and characterization of L-aspartate β-decarboxylase gene from *Alcaligenes faecalis* CCRC 11585, J. Ind. Microbiol. Biotechnol. 25 (2000) 132–140.
[17] B.N. Jones, J.P. Gilligan, *o*-Phthaldialdehyde precolumn derivatization and reversed-phase high-performance liquid chromatography of polypeptide hydrolysates and physiological fluids, J. Chromatogr. 266 (1983) 471–482.
[18] M.M. Bradford, A rapid and sensitive method for the quantitation of microgram quantities of protein utilizing the principle of protein-dye binding, Anal. Biochem. 72 (1976) 248–254.
[19] A. Lobley, L. Whitmore, B.A. Wallace, DICHROWEB: an interactive website for the analysis of protein secondary structure from circular dichroism spectra, Bioinformatics 18 (2002) 211–212.
[20] T.P. Ko, S.P. Wu, W.Z. Yang, H. Tsai, H.S. Yuan, Crystallization and preliminary crystallographic analysis of the *Escherichia coli* tyrosine aminotransferase, Acta Crystallogr. Sect. D 55 (1999) 1474–1477.
[21] T.A. Jones, J.Y. Zou, S.W. Cowan, M. Kjeldgaard, Improved methods for building protein models in electron density maps and the location of errors in these models, Acta Crystallogr. Sect. A 47 (1991) 392–400.
[22] A.T. Brunger, P.D. Adams, G.M. Clore, W.L. DeLano, P. Gros, R.W. Grosse-Kunstleve, J.S. Jiang, J. Kuszewski, M. Nilges, N.S. Pannu, R.J. Read, L.M. Rice, T. Simonson, G.L. Warren, Crystallography and NMR system: a new software suite for macromolecular structure determination, Acta Crystallogr. Sect. D 54 (1998) 905–921.